A Theoretical Study of C_2H_3ONa

Yi-Gui Wang,* Chang-Jun Sun, and Cong-Hao Deng

Institute of Theoretical Chemistry, Shandong University, Jinan, Shandong 250100, People's Republic of China

Received: June 3, 1997; In Final Form: August 27, 1997

The potential energy surface of C_2H_3ONa has been computed ab initio at the MP2/6-31+G* level of theory. The results indicate that C_2H_3ONa has three types of isomers: sodium enolate (type A), acyl sodium (type B), and α-sodium vinyl alcohol (type C). Type A isomers, for which the isomer with C_1 has the lowest in energy, are the lowest local minima on the potential energy surface. Type B isomers are weakly bound and have energies between those of type A and type C isomers. Type C isomers were found to have the highest local minima on the potential energy surface. Energy barriers between these three types of isomers are very high.

Introduction

The general formula C_2H_3ONa represents several types of organic compounds, such as enolate $CH_2{=}CH(ONa)$, acyl sodium $CH_3(C{=}O)Na$, and the model molecule of unsaturated α-sodium ether $CH_2{=}C(OH)Na$. These compounds show completely different chemical behaviors. Alkali metal enolates have long been known to be intermediates of a very large number of common and synthetically useful reactions. Different alkali metals significantly influence the structures, the aggregation condition, and the reactivity of enolates.[1,2] Many attempts have been made to change the polarity of carbonyl carbon through metallization in order to obtain useful acylation reagents (the "Grignard reagent" analogs), but acyl metals (except acyl transition metals) cannot be used in synthesis due to their instability and to the occurrence unavoidable side reactions.[3,4] However, unsaturated α-lithium ethers $CH_2{=}C(OR)Li$ are widely used as acetyl anion equivalents by virtue of their easy preparation and easy aftertreatment.[4−6] On the other hand, unsaturated α-lithium ether $CH_2{=}C(OR)Li$ can react with R′Li to replace the OR group by R′ from the opposite site of the OR group, which is a typical reaction only of carbenoids.[7−9]

Given experimental interest in this area, little theoretical work has been done on C_2H_3OM(M=alkali metals) except C_2H_3OLi. $CH_2{=}CH(OLi)$, the simplest enolate, has been briefly studied by Lynch[10] and Lambert[11] and thoroughly by us.[12] We also have studied $CH_2{=}C(OH)Li$ and $CH_3{-}C({=}O)Li$ in a previous paper,[12] in which we gave the potential energy surface of C_2H_3OLi and compared the chemistry of different isomers. Because it is very important to know how different alkli metals influence the properties of these reagents, we investigate $CH_2{=}CH(ONa)$, $CH_2{=}C(OH)Na$, and $CH_3{-}C({=}O)Na$ in this paper.

All results are compared to those of C_2H_3OLi. We have also made predictions for the C_2H_3OM (M = Li, Na, K, Rb, and Cs) series.

Computational Methods

All equilibrium geometries and transition states (TS) have been calculated using the restricted Møller−Plesset second-order perturbation (MP2) method and 6-31+G* basis sets. Vibration frequencies, also calculated at the same level of theory, have been used to characterize stationary points and to obtain zero-point energy (ZPE) corrections. The numbers of imaginary frequencies for equilibrium geometries and transition states are 0 and 1, respectively. ZPEs were not scaled. Furthermore, for comparing the role of different geometries of $CH_2{=}C(OH)Na$ in reactions, we calculated the charge on C_2 using Mulliken, natural population analysis (NPA),[13] ChelpG,[14] and MK[15] methods. All the calculations were performed with the GAUSSIAN 92 program[16] on an SGI Power Challenge M-Series workstation.

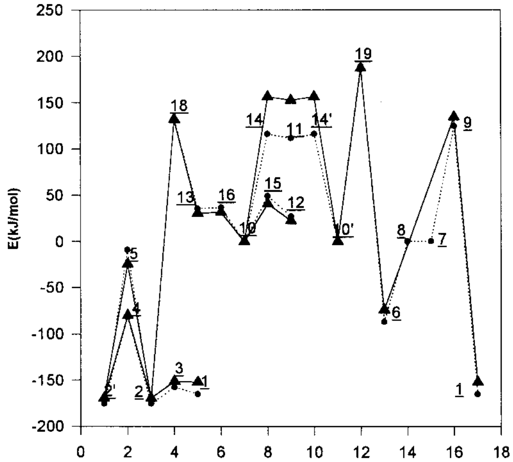

Figure 1. Profile potential energy for C_2H_3OM (M = Li, Na) (black line for M = Na, dotted line for M = Li).

Results and Discussions

I. Potential Energy Surface of C_2H_3ONa. The optimized geometries of local minima and connecting transition states connecting them are depicted separately in Figures 2, 3, and 5 for types A, B, and C isomers, respectively. Table 1 presents their total energies, zero-point vibration energies, and relative energies. Corresponding values for C_2H_3OLi are also given for comparison. Figure 1 shows the potential energy profile for the MP2/6-31+G* energies, corrected for ZPE.

As Figure 1 shows, the potential energy profile of C_2H_3ONa at MP2/6-31+G* level of theory is divided into three sections by three very high energy maxima at points 9, 18, and 19. The left section contains the isomers of sodium enolate $CH_2{=}CH(ONa)$ (type A). These have the lowest energies. The middle section contains the isomers of the molecule $CH_2{=}CNa(OH)$ (type C), which have the highest energies. Acyl sodium $CH_3C({=}O)Na$ (type B), for which point 6 is the only minimum, is in the remaining section. The sharp high points 9, 18, and 19 are transition states for interconversion of isomers of the different

S1089-5639(97)01806-9 CCC: $15.00

TABLE 1: The Total Energies, Zero Point Energies (ZPE), and Relative Energies of $C_2H_3OM^a$ (MP2/6-31+G*)

	M = Li			M = Na		
geometries	total energies E(au)	ZPE (au)	$\Delta(E+\text{ZPE})^b$ (kJ/mol)	total energies E(au)	ZPE (au)	$\Delta(E+\text{ZPE})^b$ (kJ/mol)
1	−160.256 29	0.04658	−164.9	−314.635 89	0.045 16	−152.1
2	−160.260 65	0.04688	−175.5	−314.642 88	0.045 52	−169.5
3 (TS **1-2**)	−160.252 85	0.04597	−157.5	−314.635 18	0.044 75	−151.3
4 (TS **2-2′**)	−160.222 62	0.04462	−81.6	−314.606 83	0.043 48	−80.2
5 (TS **2-2′**)	−160.196 46	0.04426	−9.0	−314.585 37	0.043 34	−24.3
6	−160.226 26	0.04623	−87.0	−314.605 80	0.044 73	−74.2
7	−160.191 57	0.04479	0.3			
8 (TS **6-7**)	−160.191 37	0.04439	−0.2			
9 (TS **1-7**)^c	−160.140 82	0.04135	124.6	−314.521 45	0.039 85	134.4
10	−160.191 48	0.04458	0	−314.576 54	0.043 75	0
11	−160.142 89	0.03847	111.5	−314.511 40	0.036 78	152.7
12	−160.181 94	0.04543	27.3	−314.568 16	0.043 94	22.5
13	−160.178 90	0.04547	35.4	−314.565 62	0.044 36	30.3
14 (TS **10-11**)	−160.141 47	0.03879	116.1	−314.510 16	0.036 88	156.2
15 (TS **10-12**)	−160.172 25	0.04404	49.1	−314.560 45	0.043 12	40.6
16 (TS **10-13**)	−160.178 13	0.04516	36.6	−314.564 65	0.043 92	31.7
17 (TS **13-13′**)	−160.160 48	0.04425	80.5	−314.547 94	0.043 28	73.9
18 (TS **2-13**)	−160.136 22	0.03980	132.6	−314.521 12	0.038 63	132.1
19 (TS **6-10**)	−160.114 06	0.03926	189.5	−314.499 89	0.038 30	186.9

[a] The data for M = Li were taken from ref 12. [b] The energy of geometry **10** is taken as zero. [c] Because the geometry **7** is not a stationary point, the geometry **9** is regarded as the transition state of **1** and **6**.

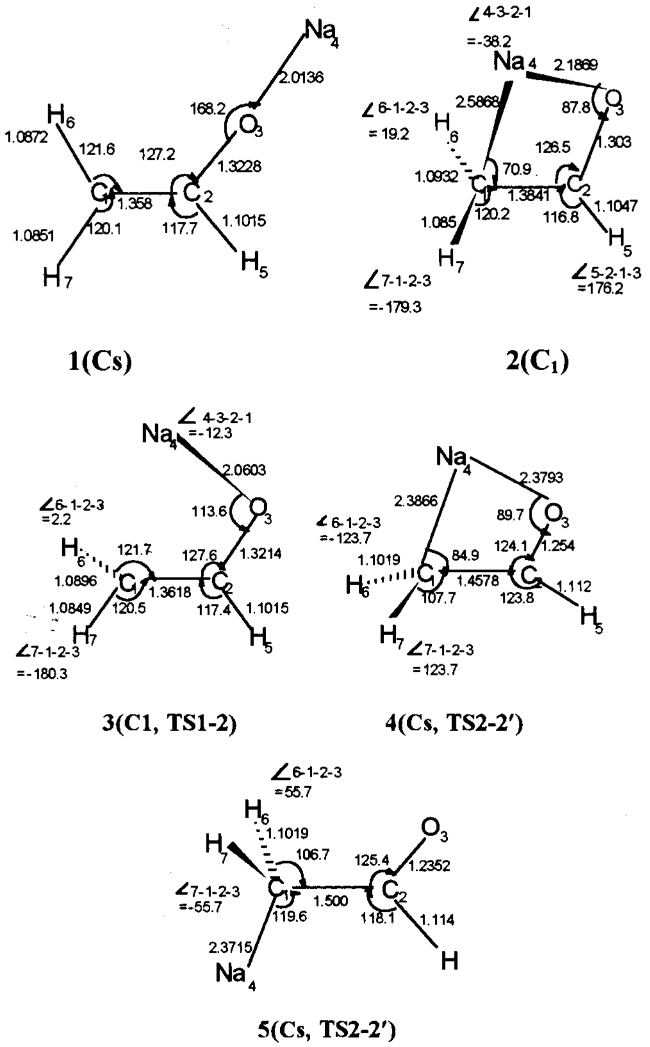

1(Cs) **2(C$_1$)**

3(C1, TS1-2) **4(Cs, TS2-2′)**

5(Cs, TS2-2′)

Figure 2. Local minima and transition states for $CH_2{=}CH(ONa)$.

types. Their heights indicate that interconversion among different types of isomers are almost impossible.

II. $CH_2{=}CH(ONa)$ (Type A)

At the MP2/6-31+G* level of theory, there are two local minima (**1** and **2**) and three transition states (3−5) (see Figure 2) on the potential energy surface of $CH_2{=}CH(ONa)$. Geometry **1** is a planar structure in which the C−O−Na group is nearly linear (bond angle =168.2°). Geometry **2** is a nonplanar structure with the sodium out of the C−C−O plane and nearly equidistant from the oxygen and the terminal carbon. The favorable energy (17.4 kJ/mol lower than geometry **1**) indicates that sodium enolates will exist in the form of geometry **2** provided that they do not aggregate. Geometry **3** is the transition state for the two local minima. This is confirmed by the single imaginary frequency of geometry **3**.

In structure **2**, Na is a chiral center. Hence, this isomer is a potentially useful template for asymmetric synthesis involving chiral nucleophiles. Two C_s symmetry geometries, **4** and **5**, are transition states between **2** and its mirror structure **2′**. The high barriers for isomerization (**4** and **5** are 89.3 and 145.2 kJ/mol higher in energy than **2**, respectively) show not only the difficulty of internal rotation but also the high order of the C−C bond. However, geometry **2** can easily isomerize to geometry **1**, which has no chiral character, through transition state **3**. The barrier for this reaction is only 18.2 kJ/mol. In practical applications, therefore, this facile isomerization should blocked by complexing geometry **2** at Na or at O.

Two differences are noteworthy when $CH_2{=}CH(ONa)$ is compared with $CH_2{=}CH(OLi)$: (1) Geometry **2** becomes more stable than geometry **1** (i.e., sodium has more tendency than does lithium to bridge O and the terminal carbon). (2) The energies of **4** and **5** become lower. This means that geometry **2** is more flexible, which in turn implies that the interaction between the positive sodium ion and the negative $CH_2{=}CH{-}O^-$ becomes weaker, making the resonance

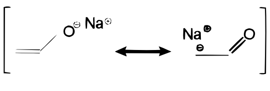

more effective.

The above trends may extend to Cs. In the sequence of substituents Li to Cs, geometry **2** becomes progressively more stable, while the C−C bond gradually loses its double-bond character.

III. R-C(=O)Na (Type B)

Calculations show that there is only one minimum (geometry **6**) on the potential energy surface of $CH_3C({=}O)Na$ (Figure 3).

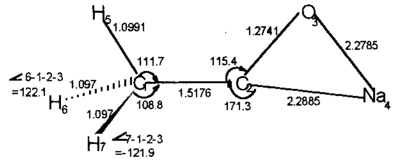

6(C$_1$)

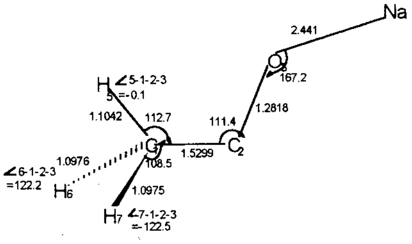

7(C$_1$)

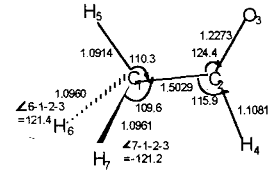

8(acetaldehyde)

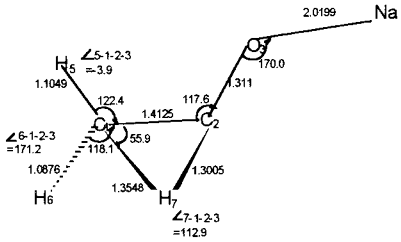

9(C$_1$,TS 6↔1)

Figure 3. Geometries for $CH_3C(=O)Na$ and acetaldehyde.

Geometry **7**, which is a real carbene, is not a local minimum at the MP2/6-31+G* level of theory. Rather, it is a point on the flat potential energy surface along the angle of CONa (see Figure 4). Compared with acetaldehyde, both the C−C and C−O bonds in geometry **6** are elongated, reflecting the weak bonding character of this isomer. Similar, even greater elongations are found in the carbene (geometry **7**). Thus, the resonance

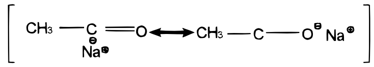

$$\left[CH_3-\underset{Na^{\oplus}}{\overset{}{\underset{\ominus}{C}}}=O \longleftrightarrow CH_3-C-O^{\ominus}Na^{\oplus} \right]$$

may still contribute to the stability of acyl sodium $CH_2-C(=O)Na$, though structure **7** is not a local minimum according to our calculations.

Through transition state **9**, a 1,2 H-migration can change geometry **6** into geometry **1**. However, the barrier is very high (208.6 kJ/mol).

Compared with acyl lithium, acyl sodium has an even longer C_1-C_2 bond (1.5176 Å for Na species and 1.5079 Å for Li species), while the C_2-O bond is shorter (1.2741 Å for Na species and 1.2807 Å for Li species). Natural orbital population analysis shows that the CH_3 group possesses more negative charge (−0.119 for acyl sodium and −0.090 for acyl lithium) while the metal possesses a little more positive charge (+0.919 for Na and +0.911 for Li). That means acyl sodium has a weaker C_1-C_2 and Na−C bonds. As a prediction for $CH_3-C(=O)M$ (M = Li, Na, K, Rb, and Cs), acyl metals will show weaker and weaker bond character (except C_2-O bond) in the sequence from Li to Cs.

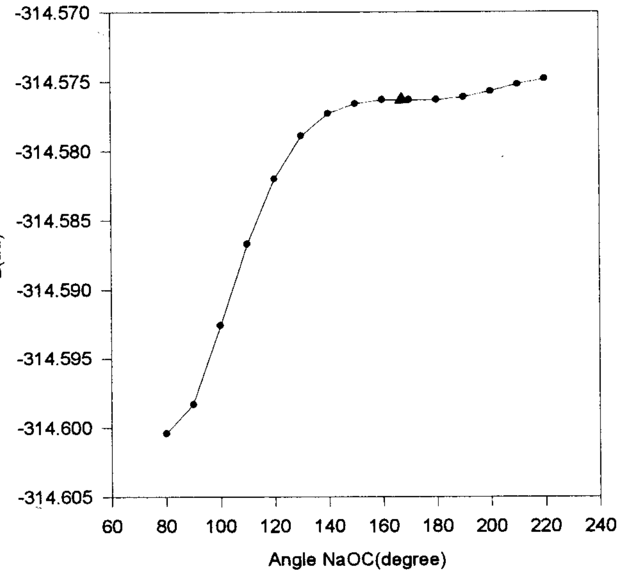

Figure 4. The energy surface along the angle NaOC.

IV. $CH_2=C(OH)Na$ (Type C)

A. Geometries and Isomerization. There are four local minima (10-13) on the potential energy surface of $CH_2=C(OH)$-Na at the MP2/6-31+G* level of theory. Three transition states (14-16) connect 10 to 11, 12, and 13, respectively. Geometry **17** is the transition state for **13** and its mirror image **13′** (see Figure 5). As an aid to comparing the role of different geometries in reaction, the dominate parts of the FMO for local minima (10-13) and for vinyldiene ($CH_2=C$:) are given in Table 3.

The carbon−oxygen-bridged isomer **10** contains a three-membered ring, in which Na^+ not only interacts with anionic C_2 but also interacts with the lone pair on oxygen. The calculations suggest that geometry **10** has a considerably longer C_2-O bond (1.4715 Å) than does vinyl alcohol (1.3722 Å). The nonbridged geometry **12**, wherein sodium is bound to the anionic carbon atom but not to oxygen, is 22.5 kJ/mol higher in energy than **10**. The short $Na-C_2$ bond (2.3046 Å), the nearly classical $\angle NaC_2C_1$ (101.5°), and the shortest C_2-O bond (1.4078 Å) among all four geometries indicate that geometry **12** is a classical structure. Geometry **13**, with the sodium ion bound only to the α-oxygen atom, is stabilized by an interaction between the lone pair of oxygen and Na^+. Geometry **13** also has a relatively longer C_2-O bond (1.4956 Å) than that in vinyl alcohol. Geometry **11**, an unsaturated metallocarbenium isomer, is rather energy-rich (152.7 kJ/mol above **10**). The existence of geometry **11** strongly indicates electrophilic character of the C_2 carbon atom. Geometries **14**, **15**, and **16** have single imaginary frequencies and are transition states for converting structure **10** to **11**, **12**, and **13**, respectively. This assertion is confirmed by the analysis of the imaginary frequency modes.

Geometry **10** is the most stable structure, and there is no doubt that it is the equilibrium geometry of $CH_2=C(OH)Na$ under general conditions, provided that $CH_2=C(OH)Na$ does not aggregate. Geometries **11** and **13** are not likely to exist, for they can very easily change into structure **10** through transition states **14** and **16**, which have energy barriers of 3.5 and 1.4

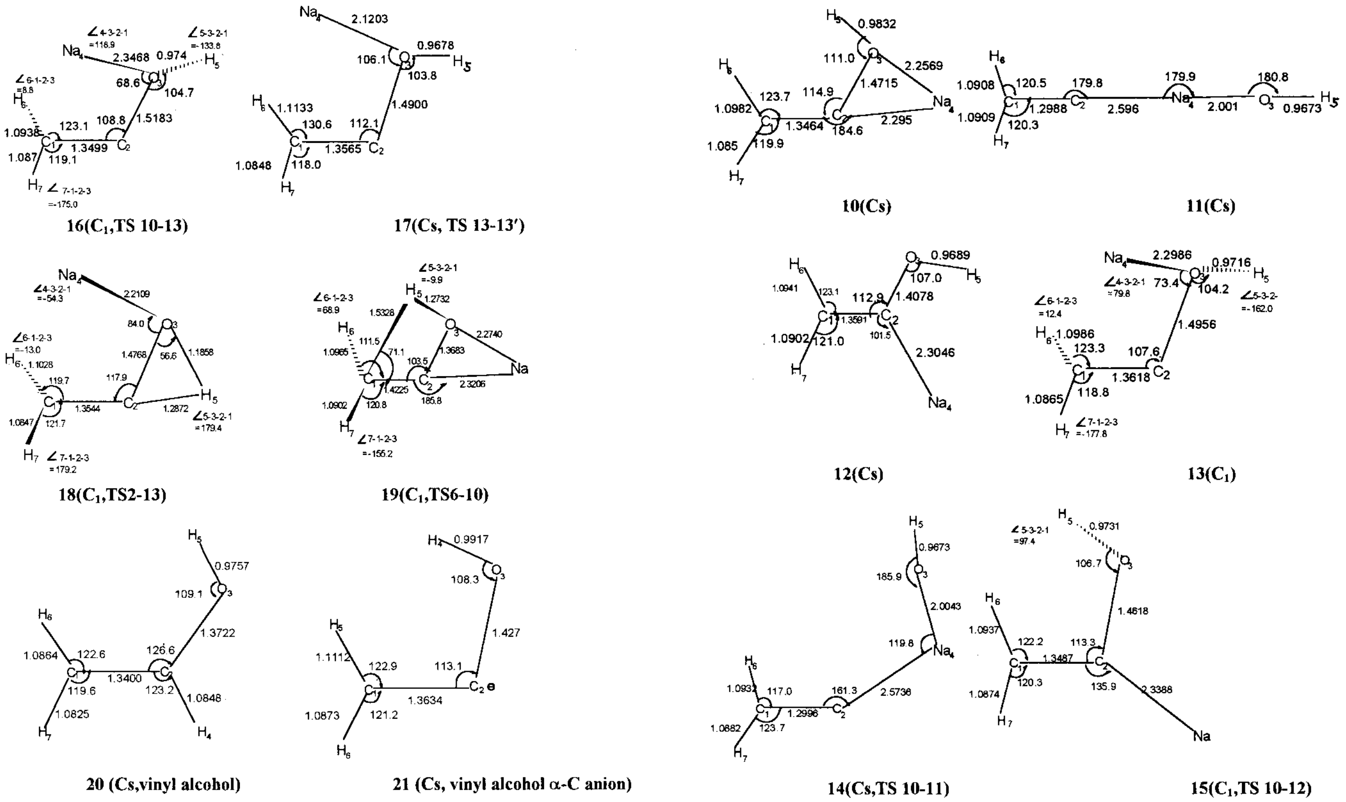

16(C_1,TS 10-13) 17(Cs, TS 13-13′) 10(Cs) 11(Cs)

18(C_1,TS2-13) 19(C_1,TS6-10) 12(Cs) 13(C_1)

20 (Cs,vinyl alcohol) 21 (Cs, vinyl alcohol α-C anion) 14(Cs,TS 10-11) 15(C_1,TS 10-12)

Figure 5. Local minima and transition states for $CH_2{=}CNa(OH)$. Geometries for vinyl alcohol and vinyl alcohol α-C anion.

TABLE 2: Net Charge on C_2 of Equilibrium Structure of $CH_2{=}C(OH)Na$ and Vinyl Alcohol α-C Anion (MP2/6-31+G*)

	geometries				
	10	11	12	13	21
Mullicken	−0.412	−0.229	−0.238	−0.484	−0.547
NPA	−0.151	+0.160	−0.190	−0.101	+0.350
CHelpG	−0.753	+0.082	−0.642	−0.747	−0.688
MK	−0.845	+0.105	−0.834	−0.830	−0.751

kJ/mol, respectively. However, $CH_2{=}C(OH)Na$ may exist in the classical form of **12**, for geometry **12** is not much higher in energy (22.5 kJ/mol higher than **10**) and is rather difficult to convert into **10** (the barrier is 18.1 kJ/mol).

Geometries **11**, **12**, and **13** can be regarded as the products of breaking either the C−O, the O−Na, or the Na−C bond of the three-member ring in geometry **10**. Because the energies decrease in the order of **14**, **15**, and **16**, it is reasonable to conclude that the C−O bond is the least likely to be broken in the reactions of α,β-unsaturated α-sodium ether.

Compared with $CH_2{=}C(OH)Li$, geometry **10** of $CH_2{=}C(OH)Na$ is easier to change into structure **13** but is more difficult to convert into **11**. As a prediction, the trend may continue down to Cs.

B. Interconversion of $CH_3C({=}O)Na$ and $CH_2{=}C(OH)Na$. When the H on O in geometry **13** moves toward the central carbon C_2 and passes the transition state **18**, geometry **2** is obtained. This process is called Wittig rearrangement if the H is replaced by an alkyl group. Because the barrier (101.8 kJ/mol) is very high, the migration of H from O to C_2 is highly unfavored kinetically.

When the H on O in geometry **10** moves toward the terminal carbon C_1 and passes the transition state **19**, geometry **6** is obtained. Neither the reaction nor the back reaction is easy to fulfill, because **19** is 261.1 and 186.9 kJ/mol higher in energy than **6** and **10**, respectively.

C. Mechanism for $CH_2{=}C(OH)Na$ To Serve as an Acyl Anion Equivalent. Geometry **13** is a special structure for two reasons: (1) FMO analysis (see Table 3) shows that the HOMO of geometry **13** has the largest electron density on C_2, though C_2 in **10** and **12** also have obvious net negative charge (see Table 2). (2) Geometry **13** has a bare C_2 that is favorable for the attack of electrophiles. However, **13** can very easily change into **10** via **16** (the barrier is only 1.4 kJ/mol), which means **13** is just a transient reactive intermediate. Thus, the reaction proceeds as follows:

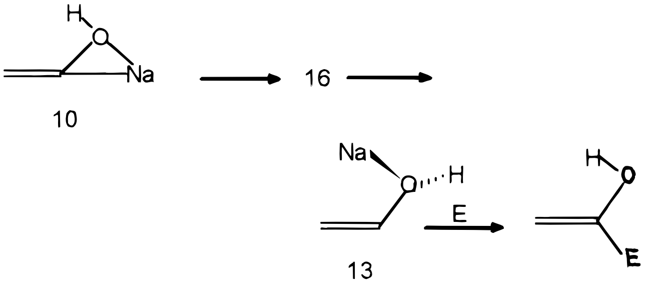

Geometry **13** is obtained from geometry **10** by the rotation of Na through transition state **16**. The attachment of electrophiles (E) to the bare anonic C_2 produces the primary product that retains the configuration at C_2.

Furthermore, geometry **13** has chiral character. It is very difficult for geometry **13** to change into its mirror image **13′** directly via transition state **17** (the barrier is 43.6 kJ/mol), but **13** can change into **10** fairly easily through transition state **16** (the barrier is 1.4 kJ/mol). Since geometry **10** has no chirality, this kind of reaction has little stereoselectivity unless oxygen is complexed with and stabilized by some group to make the second process difficult.

D. Mechanism Enabling $CH_2{=}C(OH)Na$ to React as a Carbenoid. Geometry **11** needs more attention regarding the

TABLE 3: Energies (au) and Dominate Parts of FMO for $CH_2{=}C(OH)Na$ and $CH_2{=}C:$

geometries	orbital types	orbital energies	FMO (only dominant parts given)
10	HOMO	−0.280	$+0.406C(1)(2p_z) + 0.336C(1)(3p_z) + 0.301C(2)(2p_z)$
	LUMO	−0.009	$-0.761C(1)(s) + 0.905C(2)(s) + 0.653Na(s) + 0.192Na(3s)$ $+0.255Na(4p_x) + 0.175Na(p_x) - 0.276Na(2p_y) - 0.261Na(p_y)$
11	HOMO	−0.315	$+0.596O(2s) + 0.448O(3p_x) + 0.157O(p_x)$
	LUMO	−0.002	$-0.380C(1)(p_x) + 0.386C(2)(2p_x) + 0.372C(2)(3p_x) + 0.724C(2)(p_x)$
12	HOMO	−0.270	$+0.402C(1)(2p_z) + 0.345C(1)(3p_z)$
	LUMO	−0.017	$+0.312C(1)(s)-0.375Na(4p_y) + 0.512Na(s)$
13	HOMO	−0.292	$-0.468C(1)(s) - 0.373C(2)(2p_z) + 0.375C(2)(3s) + 0.767C(2)(s)$
	LUMO	−0.013	$+0.740C(1)(s) - 0.554C(2)(s) + 0.596Na(s) + 0.419Na(4p_x)$ $+0.257Na(p_x)$
$CH_2{=}C:$	HOMO	−0.411	$+0.397C(1)(2p_x) + 0.310C(1)(3p_x) + 0.380C(2)(2p_x) + 0.226C(2)(3p_x)$
	LUMO	+0.053	$-0.401C(1)(p_y) + 0.323C(2)(3p_y) + 0.834C(2)(p_y)$

study of the mechanism enabling $CH_2{=}C(OH)Na$ to react as a carbenoid because of two reasons: (1) Net charge analysis (see Table 2) indicates that C_2 is positively charged only in geometry **11**. (2) FMO analysis shows that geometry **11** is the only structure whose LUMO is similar to that of unsaturated carbene ($CH_2{=}C:$) (see Table 3). It is reasonable to assume that geometry **11** is either the exact reactant or the structure similar to that of the transition state. However, because geometry **11** is 152.7 kJ/mol higher in energy than geometry **10**, and the energy required for **11** to turn into **10** is just 3.5 kJ/mol, it is more likely that nucleophiles react with **10** and not with **11**. Furthermore, FMO analysis indicates that a large part of the electron density resides on Na in the LUMO of geometry **10**. Thus, the reaction process will be the following:

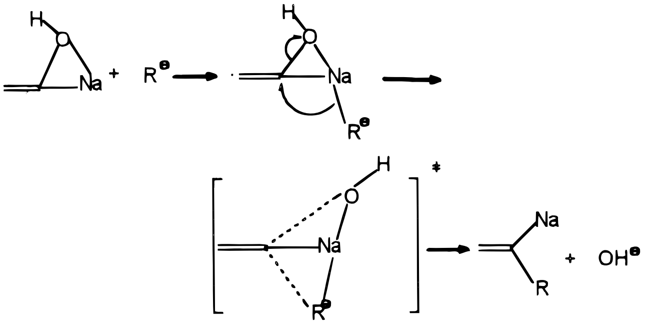

The attachment of nucleophile R^- to Na in geometry **10** forms a complex. Then, the ^-OH group is replaced by R^- through a transition state such as geometry **11** to give a product with reversion of configuration at C_2.

E. Comparison of the Two Different Mechanisms. Geometry **10** is the starting isomer for both reactions as shown above. Because geometry **10** has a larger barrier (156.2 kJ/mol) for isomerization into **11** compared to its isomerization into **13** (31.7 kJ/mol), $CH_2{=}C(OH)Na$ is more likely to react as an acyl anion equivalent than to react as a carbenoid.

Conclusions

The conclusions of this work may be summarize as follows: (1) C_2H_3ONa has three types of isomers where sodium enolate $CH_2{=}CH(ONa)$ (type A) occupies the lowest position of the PES, acyl sodium $CH_3C(C{=}O)Na$ (type B) comes in the middle, and α-sodium vinyl alcohol $CH_2{=}C(OH)Na$ (type C) takes the highest position. Barriers to interconversion among these types of isomers are very high. (2) For sodium enolate $CH_2{=}CH(ONa)$, the nonplanar structure **2** has the lowest energy and would be a useul reagent in stereoselective synthesis. (3) Acyl sodium $CH_3C({=}O)Na$ has weak bond character. A resonance form of carbene isomer **7** may contribute to the its stability. (4) Acetyl anion equivalent $CH_2{=}C(OH)Na$ has dual reactivity:

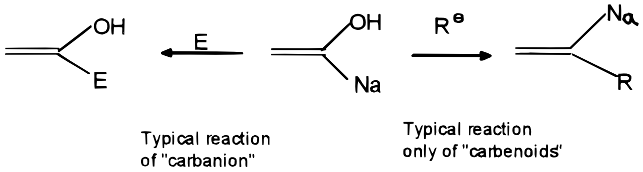

Unsaturated α-sodium substituted ether prefers reacting with electrophiles (E) to reacting with nuclephiles (such as R^-). On the one hand, the first reaction occurs by the attachment of electrophile (E) to the C_2 of geometry **13** to produce product that retains the C_2 configuration and shows little steroselectivity. On the other hand, the second reaction occurs through the replacement of attachment of ^-OH group by nuclephile (such as R^-) from the opposite site via a transition state like geometry **11**. The product of the second reaction reverses C_2 configuration. (5) After comparing C_2H_3ONa with C_2H_3OLi, we give the following predications for C_2H_3OM (M=alkali metals) series: From Li to Cs, (a) the C−C bond order of alkali metal enolates decreases, (b) acyl alkali metals have increasingly weaker bond character, and (c) $CH_2{=}C(OH)M$ becomes easier to react with electrophiles, but becomes increasingly difficult to react with nucleophiles.

We do find a transition state at RHF/6-31+G* level for reaction of $CH_2{=}C(OH)Na$ and CH_3- as follows:

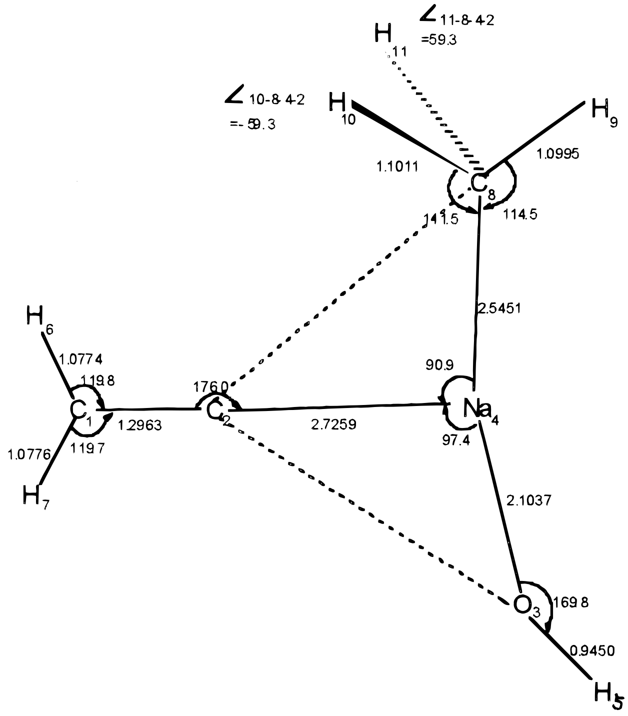

The transition state can clearly show the breaking of C_2-O_3 bond, the configuration inversion of central carbon C_2, and the connection and movement of the electron-rich CH_3 group. Detailed information concerning this reaction is to be published.

Acknowledgment. We gratefully acknowledge the National Natural Science Foundation (Grant 29773025) and the Chinese University Doctoral Foundation for the support of this work. Many thanks go to Professor George C. Schatz for his kind help with the English language.

References and Notes

(1) Jackman, L. M.; Lange, B. C. *Tetrahedron* **1977**, *33*, 2737.

(2) Seebach, D. *Angew Chem., Int. Ed. Engl*. **1988,** *27*, 1624.

(3) Chandrasekhar, J.; Andrade, J. G.; Schleyer, P. V. R.. *J. Am. Chem. Soc.* **1981**, *103*, 5612.

(4) Seebach, D. *Angew Chem., Int. Ed. Engl*. **1969,** *8*, 639.

(5) Schöllkopf, U.; Hänssle, P. *Justus Liebigs Ann. Chem.* **1972**, *763*, 208.

(6) Baldwin, J. E.; Höfle, G. A.; Lever, O. W., Jr. *J. Am. Chem. Soc.* **1974**, *96*, 7125.

(7) Stang, P. J. *Acc. Chem. Res.* **1978**, *11*, 107.

(8) Schöllkopf, U. *Angew Chem., Int. Ed. Engl*. **1970**, *9*, 763.

(9) Boche, G.; Lohrenz, J. C. W.; Opel, A. *Lithium Chemistry: A Theoretical and Experimental Overview*; Spase, A.-M., Schleyer, P. V. R., Eds.; John Wiley and Sons, Inc.: New York, 1995; pp 209−215.

(10) Lynch, B. J.; Newcomb, M.; Bergbreiter, D. E.; Hall, M. B. *J. Org. Chem.* **1980**, *45*, 5005.

(11) Lambert, C.; Wu, Y.; Schleyer, P. V. R. *J. Chem. Soc., Chem. Commun.* **1993**, 255.

(12) Wang, Y. G.; Sun, C. J.; Deng, C. H. *J. Mol. Struct. (THEOCHEM)* **1998**, *429*, 207.

(13) Reed, A. E.; Carpenter, J. E.; Wienhold, F. NBO Version 3.1; Gaussian, Inc.: Pittsburgh, 1992.

(14) Breneman, C. M.; Wiberg, K. B. *J. Comput. Chem*. **1990**, *11*, 361.

(15) Besler, B. H.; Merz, K. M.; Kollman, P. A. *J. Comput. Chem*. **1990**, *11*, 431.

(16) Frisch, M. J.; Trucks, G. W.; Head-Gordon, M.; Gill, P. M.; Wong, W. W.; Foresman, J. B.; Johnson, B. G.; Schlegel, H. B.; Robb, M. A.; Replogle, E. S.; Gomperts, R.; Andres, J. L.; Ragharachari, K.; Binkley, J. S.; Gonzalez, C.; Martin, R. L.; Fox, D. J.; Defrees, D. J.; Baker, J.; Stewart, J. J. P.; Pople, J. A., Gaussian 92, Revision F.4; Gaussian, Inc.: Pittsburgh, PA, 1992.